Wall Shear Rates Generated during Coalescence of Pendant and Sessile Drops

Praveen M. Somwanshi*, K. Muralidhar and Sameer Khandekar

Department of Mechanical Engineering,
Indian Institute of Technology Kanpur, Kanpur 208016 India

(*Corresponding author, e-mail: praveens@iitk.ac.in)

Keywords: Pendant and sessile drops, Coalescence, Three phase contact line, Bridge formation, Wall shear stress

Abstract Coalescence is the process by which two or more drops contact each other and merge to form a single daughter drop. It may occur in a fluid medium or on a solid surface. In both instances, coalescence is an intense dynamic process during which the fluid is momentarily set into motion. The present study compares the shear rates, and hence, shear stresses generated on the wall because of the coalescence of two drops in pendant and sessile configurations. In experiments, two drops of equal volume are placed adjacent to each other till a liquid bridge is formed with the drops just touching each other. The equilibrium contact angle is 110^o. Fluids considered are water on and underneath a textured surface. Coalescence is driven by the negative curvature at the liquid bridge. The contact line moves and bridge relaxes as flow takes place from a region of higher to lower pressure. The entire process has been imaged by using a high speed camera. The image sequence is analyzed to find the instantaneous center of mass of the drop, which in turn, yields the velocity components. These are used to find the time-dependent wall shear rates. Experiments show that two timescales appear during the merging of the drops. Large shear stresses are momentarily developed at the wall with a magnitude that depends on the drop volume. Oscillations are stronger in the pendant configuration where gravity is an additional driving force.

1 Introduction

The discussion here is on the merger of two small liquid drops located on a textured partially-wetting surface. Such a configuration is encountered during dropwise condensation of vapor on a cooler substrate. The drops are not pinned at the three-phase contact line and the footprint of the coalesced drop evolves with time. The coalescence process is responsible for introducing an additional velocity in the liquid mass, length scale due to merger, and timescales due to release and dissipation of excess surface energy.

adfa, p. 1, 2011.

Andrieu et al. [1] studied the time required for coalescence of sessile water drops over a plane surface in the contact angle range of 30-50°. Aryafar et al. [2] studied coalescence of a moving drop at the interface of two immiscible liquids. Blanchette and Bigioni [3] simulated a liquid drop coalescing with a reservoir of an identical liquid. Bordoloi and Longmire [4] studied coalescence of a liquid drop at the interface of two liquids, the one below being identical to the drop. In experiments, the thin film at the periphery of the drop was seen to rupture at its thinnest point leading to rapid collapse of the drop. Graham et al. [5] experimentally studied impact of a falling drop with another placed on a horizontal surface. The surface texture was varied, ranging from hydrophilic to hydrophobic. Narhe et al. [6] compared coalescence induced in sessile drops deposited by a syringe as opposed to drops grown by condensation. From experiments over superhydrophobic surfaces, Rykaczewski et al. [7] showed that coalescence can lead to the formation of micro- and nano-scaled satellite drops that are swept away by the primary drops before they can occupy nucleation sites during dropwise condensation. Sprittles and Shikhmurzaev [8] suggested that the initial coalescence mechanism of two freely suspended drops involves trapping of the free surface within, followed by a gradual disappearance of the internal interface, as opposed to a bridge formation. Thorodddsen et al. [9] demonstrated bridge formation at the interface of a pendant and a sessile drop using ultra-high speed imaging. Wu et al. [10] studied surface-tension controlled coalescence of drops facing each other and examined bridge formation at the interface.

It is now understood that drops merge with the formation of a bridge between the respective liquid interfaces. The bridge evolves in time, eventually leading to a unified interface of the combined droplet. The liquid velocities generated at this early stage, in conjunction with the excess available free energy due the coalescence, may deform the interface further. The magnitude of initial velocity generated depends on the internal pressure difference across the drops. Thus, factors such as drop volume and contact angle, which dictate the interface curvature, become determining factors at early times, immediately following coalescence. On a long term basis, the contact angle at the three-phase contact line will approach the equilibrium value, while bulk fluid motion generated due to excess free energy gets dissipated by viscosity. The total time for post-coalescence equilibrium will, usually, correspond to the timescale of bridge growth added to the timescale of relaxation – either in the bulk by viscosity or dissipation at the three-phase contact line due to its motion in the process of reaching the new equilibrium.

Coalescing liquid drops experience a variety of forces whose relative magnitudes change with time. These forces are related to surface tension, gravity, viscosity, and inertia. Derived quantities such as pressure are decided by these primary forces. The ratio of a pair of forces will generate dimensionless parameters that delineate the relevant limiting mechanisms. Apart from fluid and interfacial properties, the drop size is an important parameter. It is to be expected that surface tension would be strong particularly in comparison to gravity and inertia forces when the drop dimension is small. Though not distinguishable in terms of dimensionless parameters, gravity forces are expected to be more important for pendant drops than sessile. In the following discussion, the drops are taken to merge under ambient conditions. Hence, surface tension

would be that appearing at the liquid-air interface. Further, density difference between the two is practically equal to the liquid density.

The following section describes experiments for the coalescence of equal volume water drops (1 to 3.5 µl) in pendant and sessile configurations when the equilibrium contact angle is close to 110°.

2 Experimental arrangement

Figure 1 shows the schematic drawing of an experimental set-up developed as a part of this work. It is used to place and image one or more drops on a horizontal surface in pendant and sessile configurations. The merging drops are imaged in a vertical plane using a high speed camera whose viewing axis is horizontal. A micro liter syringe with 100 µL capacity and a least count of 0.02 µL is used to deposit sessile/pendant drops above or on the underside of the substrate. The substrate is prepared using chemical texturing and equilibrium contact angle for water on this surface was measured to be 110^o ($\pm 2^o$). The substrate is vacuum dried before each experiment to ensure repeatability of the coalescence sequence. The drops were illuminated by a white LED source. A monochrome high speed camera (Photron FASTCAM SA-3), 4000 frames per second, 6 bit digitization, was used for recording the image sequence (Figures 2-3).

Precautions required in experiments include maintaining surface quality, alignment, and cleanliness so that the initial and final equilibrium contact angles are identical for all drop volumes. For this purpose, surfaces were not re-used and a new textured substrate was formed for each experiment. Coalescence was carefully initiated without impact by increasing the volume of one of the drops using the syringe. For certain under-prepared surfaces, pinning was observed and the data recorded in such experiments were discarded. Post coalescence, the original contact angle recovered over a period of several seconds to a minute; this long-time data is not shown in the images of Figures 2-3.

Figure 2(a) shows an image sequence of coalescing drops as seen in the front-view for pendant drops of equal volumes (=1.3 µl). Figure 2(b) shows a companion image sequence of coalescing drops for sessile drops of equal volumes (=1.5 µl). Figure 3(a) is an image sequence for larger pendant drops of equal volumes (=3.1 µl). Figure 3(b) is a companion plot for sessile drops of equal volumes (=3.5µl). The footprint of two coalescing drops, 0.03 µl each was imaged using a high resolution confocal microscope (Leica CTR6500). A time sequence of the footprint thus recorded is shown in Figure 4. Footprints of larger drops could not be obtained with the available confocal microscope.

For distance measurement, the camera was calibrated in the *x*- and the *y*-directions before starting the experiment. Since measurements were intended to track the movement of the centroid, the focusing plane was selected as the mid-plane of the merging drops.

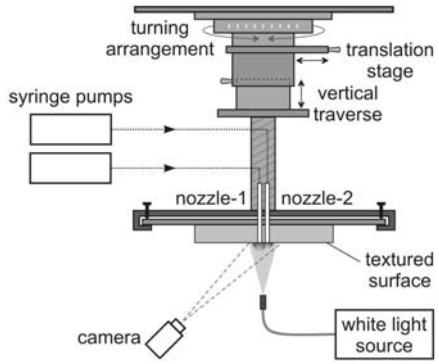

Fig. 1: Schematic drawing of the experimental set-up when two pendant drops are imaged

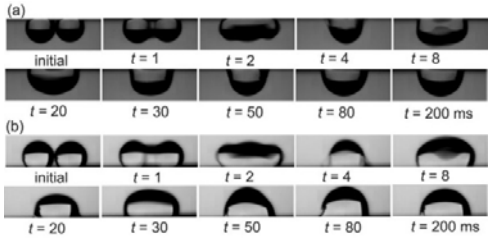

Fig. 2: Image sequence of coalescence for (a) pendant drops of nearly equal volume (v_1 = 1.3 µl v_2 = 1.2 µl) and (b) sessile drops (v_1 = 1.5 µl v_2 = 1.4 µl)

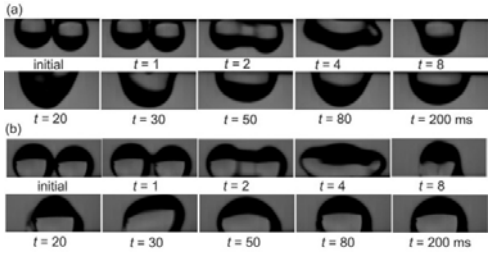

Fig. 3: Image sequence of coalescence for (a) pendant drops of nearly equal volume (v_1 = 3.1 µl v_2 = 2.8 µl) and (b) sessile drops (v_1 = 3.5 µl v_2 = 3.4µl)

In Figures 2-4, small and long timescales are clearly visible. The initial timescale of 0-10ms is for bridge formation during which the drops lose their identity. The second, the relaxation timescale (~ 200ms), is when the velocities generated within dissipate by viscosity. In the following discussion, the movement of centroids of the merging drops, velocities acquired, and shear rates are plotted as a function of time.

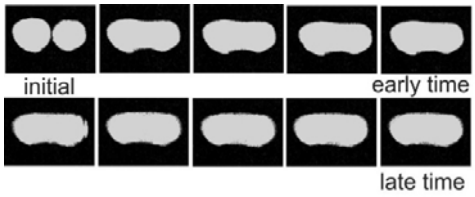

Fig. 4: Footprint of coalescence of pendant drops of equal volume (v_1 = 0.03 µl v_2 = 0.03 µl) on a Teflon substrate with an equilibrium contact angle of 90°

2.1 Image analysis

From images, *x*- and *y*-components of the centroid are calculated from the image with *N* pixels as

$$x_c = \frac{\sum_{i=1}^{N} x_i \cdot \gamma_i}{\sum_{i=1}^{N} \gamma_i} \quad y_c = \frac{\sum_{i=1}^{N} y_i \cdot \gamma_i}{\sum_{i=1}^{N} \gamma_i} \tag{1}$$

Here, $\gamma_i = 1$ inside the drop and $\gamma_i = 0$ outside the drop. The *x*- and *y*-components of centroid for a pair of images yield velocity components

$$u_c = \frac{(x_c)_{i+1} - (x_c)_i}{t_{i+1} - t_i} \quad v_c = \frac{(y_c)_{i+1} - (y_c)_i}{t_{i+1} - t_i} \tag{2}$$

The *x*-component and the *y*-component of centroid velocities can be combined with the definition of shear rate

$$\dot{\gamma} = \left| \frac{\partial u_c}{\partial y_c} + \frac{\partial v_c}{\partial x_c} \right| \tag{3}$$

The shear rate at the wall can be approximately estimated as

$$\dot{\gamma} \approx \frac{(u_c)_i}{(y_c)_i} \tag{4}$$

To understand the forces of relevance in the present set of experiments, one can define the characteristic length scale as

$$L = (V_D)^{1/3} \tag{5}$$

The characteristic velocity based on gravity forces and surface tension are respectively defined as

$$U = \sqrt{gL} \text{ and } U = \sqrt{\frac{\sigma}{gL}} \tag{6}$$

The following dimensionless numbers can now be obtained:

$$Bo = \frac{\rho g L^2}{\sigma} \quad Oh = \frac{\mu}{\sqrt{\rho \sigma L}} \quad \mathrm{Re} = \frac{\rho U L}{\mu} \tag{7}$$

Typical values of these dimensionless quantities for the drop sizes considered are given in Table 1. The Bond number is a ratio of gravity to surface tension; Ohnesorge

number (*Oh*) is viscous to surface tension; Reynolds number scales inertia with the viscous. When Bond number is small (< 1), surface tension is significant. For *Bo*=1, *L* is capillary length of the problem, being 3mm for the present study. Hence, surface tension is relevant in experiments discussed in the following sections.

Table 1. Range of non-dimensional numbers for volumes considered in the present experiments. *Bo* is Bond number, *Oh* is Ohnesorge number, and Re is Reynolds number. Since *Bo*< 1, surface tension is important in all the experiments. Since *Oh* is much smaller than unity, viscosity plays a smaller role indicating a long relaxation process. In contrast, gravity is a relevant force of interest. Reynolds number being large, oscillations persist because of inertia-gravity coupling.

Water (25°C and 1 atm.)	
d = 0.5 - 3 mm	
L = 0.4 – 2.4 mm	Bo = 0.022 – 0.783
	Oh = 0.0053 – 0.002
$U = \sqrt{gL}$ 0.063 – 0.153 m/s	$U = \sqrt{\frac{\sigma}{gL}}$ 0.173 – 0.425 m/s
Re = 25 – 365	Re = 68 – 1014

3 Results and Discussion

Internal pressure is larger in small drops and is balanced by interfacial tension and weight. Internal pressure diminishes in drops of larger volumes. The pressure difference between adjacent drops of equal volume will be small and is determined by the curvature of the bridge joining them. Soon afterwards, a single drop is formed and internal pressure will scale with the new volume of the combined drop. Pressure difference related to the bridge curvature will, however, set the fluid in motion. It is to be expected that larger velocities in the *x*-direction are initially obtained at lower volumes. These would decay faster as well, in smaller drops. In the pendant mode, gravity and pressure are opposed to each other, pressure differences are small and the resulting velocities (and displacements) are also smaller. Oscillations are influenced by gravity and will depend on the centroid displacement in the vertical direction, being larger in drops of larger volume. The shear rate is proportional to the *x*-component velocity parallel to the surface and inversely to the normal distance of the centroid from the wall. Hence, sessile drops generate greater shear in the long timescale (of > 100ms), though the short timescale (< 10ms) shear rates are uniformly large. Velocities generated in coalescing drops in the sessile and pendant modes are discussed in the following sections.

3.1 Coalescence of drops of smaller volume

Figure 5(a) shows variation of the *x*-component of the centroid with time when drop volumes are in the range of 1- 1.5 µl. Its maximum value is 0.16 mm in the pendant mode and 0.27 mm in the sessile, both occurring at short time. Figure 5(b) shows variation of the *y*-component of the centroid with time. The maximum vertical displacement of the centroid is 0.18 mm in the pendant configuration and 0.2 mm in the sessile. Figure 5(c) shows variation of the *x*-velocity with time and Figure 5(d) shows the variation of the *y*-velocity with time. The maximum *y*-component velocity is 180 mm/s in the pendant configuration and 120 mm/s in the sessile. Figure 5(e) presents the shear rate variation with time. Soon after bridge formation, shear rates in the pendant mode fade away in comparison to the sessile. This trend is related to a larger pressure difference arising in sessile drops compared to the pendant where part of the pressure difference is cancelled by gravity.

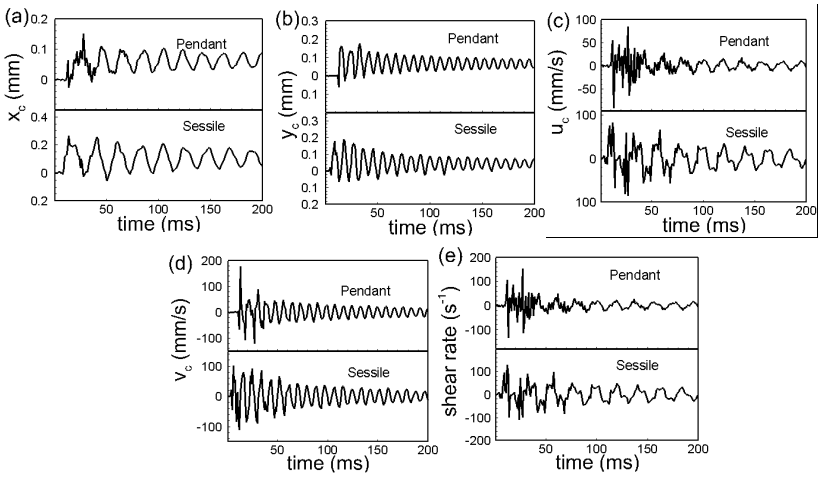

Fig. 5: Coalescence of pendant drops of equal volumes (v_1 = 1.3 µl v_1 = 1.2 µl) and sessile drops for equal volumes (v_1 = 1.5 µl v_1 = 1.4 µl) showing time-variation of (a) *x*-component of centroid, (b) *y*-component of centroid, (c) *x*-component of centroid velocity, (d) *y*-component of centroid velocity, and (e) shear rate. Coordinates *x* and *y* are shown relative to the initial centroid positions of the individual drops.

3.2 Effect of volume

At higher volumes, the difference between the equilibrium drop shapes in the sessile and the pendant modes is greater with the centroid of an equilibrium pendant drop moving away from the solid substrate. In addition, larger drops have a smaller internal pressure and the horizontal velocity components generated during coalescence are smaller. In contrast, vertical oscillations in the pendant mode can be expected to be marginally stronger. Overall, larger drops are likely to produce smaller shear rates.

Between Figures 5 and 6, differences are not substantial because the length scales of 1 and 3 µl drops are fairly close.

Figure 6(a) shows the variation of the *x*-component of the centroid with time when the drop volumes are in the range of 3- 3.5 µl. Its maximum value is 0.36 mm in the pendant mode and 0.66 mm in the sessile. Figure 6(b) shows variation of the *y*-component of the centroid with time. The maximum vertical displacement of the centroid is 0.26 mm in the pendant configuration and 0.32 mm in the sessile. These maxima occur at early times during bridge formation. Figure 6(c) shows variation of the *x*-velocity with time and Figure 6(d) shows the variation of the *y*-velocity with time. The maximum *y*-component velocity is 160 mm/s in the pendant configuration and 200 mm/s in the sessile. Figure 6(e) presents the shear rate variation with time. During the relaxation phase, velocities and shear rates are generally higher for the sessile as opposed to the pendant arrangement. The difference arises from larger pressure differences in sessile drops whereas in the pendant configuration, pressure is partially compensated for by gravity. For larger volumes, centroid displacement is larger and contributes to smaller shear rates. A larger volume is indicative of prolonged inertial as well as gravitational oscillations with lower levels of viscous relaxation. These trends are not sharply brought out because surface tension continues to be a dominant restoring force for drop volumes in the range of 1-3.5 µl.

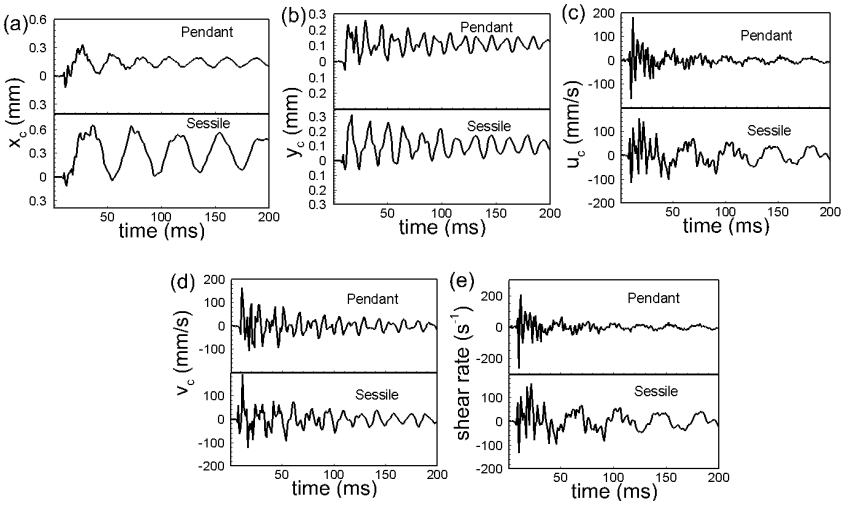

Fig. 6: Coalescence of pendant drops of larger volumes (v_1 = 3.1 µl v_1 = 2.8 µl) and sessile drops of larger volumes (v_1 = 3.5 µl v_1 = 3.4 µl) showing the time-variation of (a) *x*-component of centroid, (b) *y*-component of centroid, (c) *x*-component of centroid velocity, (d) *y*-component of centroid velocity, and (e) shear rate. Coordinates *x* and *y* are shown relative to the initial centroid positions of the individual drops.

For sessile and pendant drops, Figs. 5 and 6 show that the time period of oscillations in the *x*-velocity is greater than the *y*. This is because the former is pressure dri-

ven while the latter is related to gravity. Both time periods are greater for larger drops. The initially obtained large velocities in all configurations are of comparable magnitude showing that viscosity as well as gravity plays only a secondary role. The *x*-component velocity in a sessile arrangement is greater than the pendant but the *y*-component velocity are similar. The higher persistent shear rates in sessile drops during the relaxation mode, compared to the pendant, are related to higher *x*-velocities and smaller vertical displacement of the centroid.

4 Conclusions

Coalescing water drops deposited on a chemically textured surface in pendant and sessile configurations were imaged and analyzed. An initial bridge formation over a shorter timescale followed by a long relaxation process was seen for both arrangements. Large shear rates are momentarily generated for sessile and pendant drops that decay over time. Long term behavior of coalescence shows the following trends for the two drop volumes studied.

1. The *x*-component centroid movement is more perceptible in sessile drops compared to the pendant. The *y*-component centroid movement is larger for a pendant drop.
2. The time periods of *x*-velocity oscillations of a sessile drop are greater than the pendant while those of the *y*-component are comparable.
3. Shear rate oscillations of sessile drops are larger than the pendant.
4. The difference between shear rates in pendant and sessile arrangements is more prominent in larger drops.

Nomenclature

d_1	Diameter of bigger drop (m)
d_2	Diameter of smaller drop (m)
$\vec{g}$	Acceleration due to gravity (m/s^2)
L	Characteristic dimension (m)
m	Mass of drop (kg)
N	Number of pixels
t	Time (s)
U	Characteristic velocity (m/s)
u_c	*x*-component of centroid velocity (m/s)
V	Volume of drop (m^3)
v_c	*y*-component of centroid velocity (m/s)
V_D	Volume of composite drop (m^3)

x_c *x*-coordinate of centroid (m)

y_c *y*-coordinate of centroid (m)

γ Area function

μ Dynamic viscosity of fluid (Pa-s)

ρ Density of fluid (kg/m^3)

σ Surface tension (N/m)

References

1. Andrieu, C., Beysens, D. A., Nikolayev, V. S., and Pomeau, Y., 2002. Coalescence of sessile drops, *J. Fluid Mech.* 453 427-438.
2. Aryafar, H. and Kavehpour, H. P., 2006. Drop coalescence through planar surfaces, *Phys. Fluids* 18 072105.
3. Blanchette, F. and Bigioni, T.P., 2009. Dynamics of drop coalescence at fluid interfaces, *J. Fluid Mechanics*, 620, 333-352.
4. Bordoloi, A. D. and Longmire, E. K., 2012. Effect of neighboring perturbations on drop coalescence at an interface, *Phys. Fluids* 24 062106.
5. Graham, P.J., Farhangi, M.M. and Dolatabadi, A., 2012. Dynamics of droplet coalescence in response to increasing hydrophobicity, *Phys. Fluids* 24, 112105.
6. Narhe, R., Beysens, D., and Nikolayev, V. S., 2004. Contact line dynamics in drop coalescence and spreading, *Langmuir* 20(4) 1213-1221.
7. Rykaczewski, K., Scott, J.H.J., Rajauria, S., Chinn, J., Chinn, A.M., and Jones, W., 2011. Three dimensional aspects of droplet coalescence during dropwise condensation on superhydrophobic surfaces, *Soft Matter*, 7, 8749-8752.
8. Sprittles, J.E. and Shikhmurzaev, Y.D., 2012. Coalescence of liquid drops: Different models versus experiment, *Phys. Fluids*, 24, 122105.
9. Thoroddsen, S. T., Takehara, K., and Etoh, T. G., 2005. The coalescence speed of a pendent and a sessile drop, *J. Fluid Mech.* 527 85–114.
10. Wu, M., Cubaud, T., and Ho C. M., 2004. Scaling law in liquid drop coalescence driven by surface tension, *Phys. Fluids* 16 L51.